applied sciences

MDPI

Article

Hydrogen Storage in Propane-Hydrate: Theoretical and Experimental Study

Mohammad Reza Ghaani [1,*], Satoshi Takeya [2] and Niall J. English [1,*]

[1] School of Chemical and Bioprocess Engineering, University College Dublin, Belfield, 4 Dublin, Ireland
[2] Research Institute for Material and Chemical Measurement, National Institute of Advanced Industrial Science and Technology (AIST), Tsukuba 305-8565, Japan; s.takeya@aist.go.jp
* Correspondence: mohammad.ghaani@ucd.ie (M.R.G.); niall.english@ucd.ie (N.J.E.); Tel.: +353-1-7161758 (M.R.G.); Fax: +353-1-7161177 (N.J.E.)

Received: 29 October 2020; Accepted: 10 December 2020; Published: 15 December 2020

Abstract: There have been studies on gas-phase promoter facilitation of H_2-containing clathrates. In the present study, non-equilibrium molecular dynamics (NEMD) simulations were conducted to analyse hydrogen release and uptake from/into propane planar clathrate surfaces at 180–273 K. The kinetics of the formation of propane hydrate as the host for hydrogen as well as hydrogen uptake into this framework was investigated experimentally using a fixed-bed reactor. The experimental hydrogen storage capacity propane hydrate was found to be around 1.04 wt% in compare with the theoretical expected 1.13 wt% storage capacity of propane hydrate. As a result, we advocate some limitation of gas-dispersion (fixed-bed) reactors such as the possibility of having un-reacted water as well as limited diffusion of hydrogen in the bulk hydrate.

Keywords: hydrogen storage; hydrogen/propane hydrate; molecular dynamics; cage occupancy

1. Introduction

Hydrogen is considered as an efficient, operationally convenient, and cost-effective energy resource for a clean future. These features of hydrogen have introduced hydrogen production and hydrogen storage techniques as an attractive field of study. In this regard, it is necessary to leverage and understand the full benefits of hydrogen application in the context of "Hydrogen Economy". For instance, the excess H_2 generated from other renewable energy resources such as solar energy and wind provide a wide range of economically efficient in possibilities in a "power-to-gas" vision.

Clathrate hydrates, also known as gas hydrates, are composite compounds, in which water molecules form a lattice framework that are entrapped guest molecules in. This family of materials crystalize in three main structures [1]: types sI, sII and sH. Each polymorph is made by a different number of water molecules which form a different number of cages. For example, dual propane/hydrogen hydrate with sII type structure has a unit cell 136 water molecules form eight $5^{12}6^4$ and sixteen 5^{12} cavities. Propane can only be fitted in large ($5^{12}6^4$) cavities, while smaller 5^{12} cages are empty and have potential to entrap other small guest molecules, e.g., H_2, for physical gas storage application [2].

Hydrogen hydrate crystallises in sII type hydrate form and at maximum can store hydrogen equivalent to 5.3 wt% of its total mass (mass H_2 per mass H_2O) sII at 250 K and 2–3 kbar pressure [3,4]. Indeed, this high-pressure demand acting as a limiting constraint on its practical application as a hydrogen-storage medium [5–7]. To solve this issue one approach can be employing binary hydrates with a "helper" molecule (liquid or gas) and hydrogen as the secondary compound, those are stable at milder conditions, e.g., at ~30–50 bar and ~280 K but with a substantially lower hydrogen-storage capacity [5–9].

Apart from well-studied liquid-phase promoters such as THF hydrate [8–10] for sII H_2-bearing hydrates, there have been studies on gas-phase promoters facilitation sII H_2-containing clathrates. Hasegawa et al. investigated the possibility of having SF_6 as the helper compound in forming sII hydrate while hydrogen molecules can be stored in small cages. In their molecular simulation study, they have observed frequent diffusion of H_2 molecules between large cages, however, having SF_6 molecules in the large cages are limiting the diffusion. They proposed an optimal occupancy of large cages with SF_6 in which hydrate can stay stable while the maximum H_2 storage capacity can be obtained [11]. Skiba et al. found sII structured propane-/hydrogen-mixed hydrate to be favourable for storing hydrogen with 0.33 wt% capacity at 270 K and 120 bar [12].

In the present study, we have investigated H_2- uptake and release kinetics through non-equilibrium molecular dynamics simulations at various temperatures, as well as experimentally forming propane hydrate and evaluating the experimental capacity of hydrogen storage into the formed propane hydrate.

2. Simulation Methodology

In this study, the mixed hydrogen-/propane- clathrate was stimulated by pairwise potentials; TIP4P/2005 type models for water "which have been used in many simulation studies on hydrates" [13]. Using TIP4P/2005, Huang et al. showed an accurate sequence of energies in addition to structural parameters for ice polymorphs, in agreement with dispersion-corrected Density Functional Theory (DFT) [14]. In our previous recent studies [15–17], we showed the melting point of propane and propane/hydrogen hydrate can be predicted close to their experimental values using TIP4P/2005 potential. the General Amber Force Field (GAFF) used to handle Propane [18] and restrained electrostatic potential atomic partial charges (RESP) were sampled for propane from the HF/6-31G(d) electrostatic potential [19]. The model proposed by Alavi et al. was used to parametrise the hydrogen molecules [20]. Smooth particle-mesh Ewald method [21] was applied for long-range electrostatic and the temperature was controlled using Nosé–Hoover-thermostat [22]. Initial coordinates of oxygen atoms in sII-clathrate unit cells were constructed from X-ray diffraction data [23]. The unit-cell lengths were 17.32 Å; initial orientations of water molecules were chosen by the Rahman–Stillinger procedure [24] to comply with Bernal–Fowler rules [25] and have a negligible total-system dipole moment.

The simulations were done for both uptake and release of hydrogen into/from propane hydrate. A $2 \times 2 \times 2$ supercell was constructed and was put in contact in the + and $-x$-directions with the length of ~129.75 each direction by vacuum. For the release simulation, every large cage was occupied by one propane molecule, while one hydrogen molecule located in every small one. The vacuum part is large enough to not avoid any significant pressure built up during the time of the hydrogen release process. In the case of uptake study, the same $2 \times 2 \times 2$ supercell loaded only with propane molecules in large cages and keeping the small cages empty was sandwiched between relaxed hydrogen molecules with the length of 36 Å along the ± X-axis (i.e., a total hydrogen-phase length of 72 Å). Assuming the hydrogen molecules as idea gas, the added hydrogen molecules can provide a pressure around 1000 bar at 273 K in the gas area. To afford compatibility with experimental data (in which case the cages at the interface are, ipso facto, complete before any thermal-imposed decomposition for heating above the melting temperature), extra water molecules were added to have complete cages at the interface [15]; cf. Figure 1.

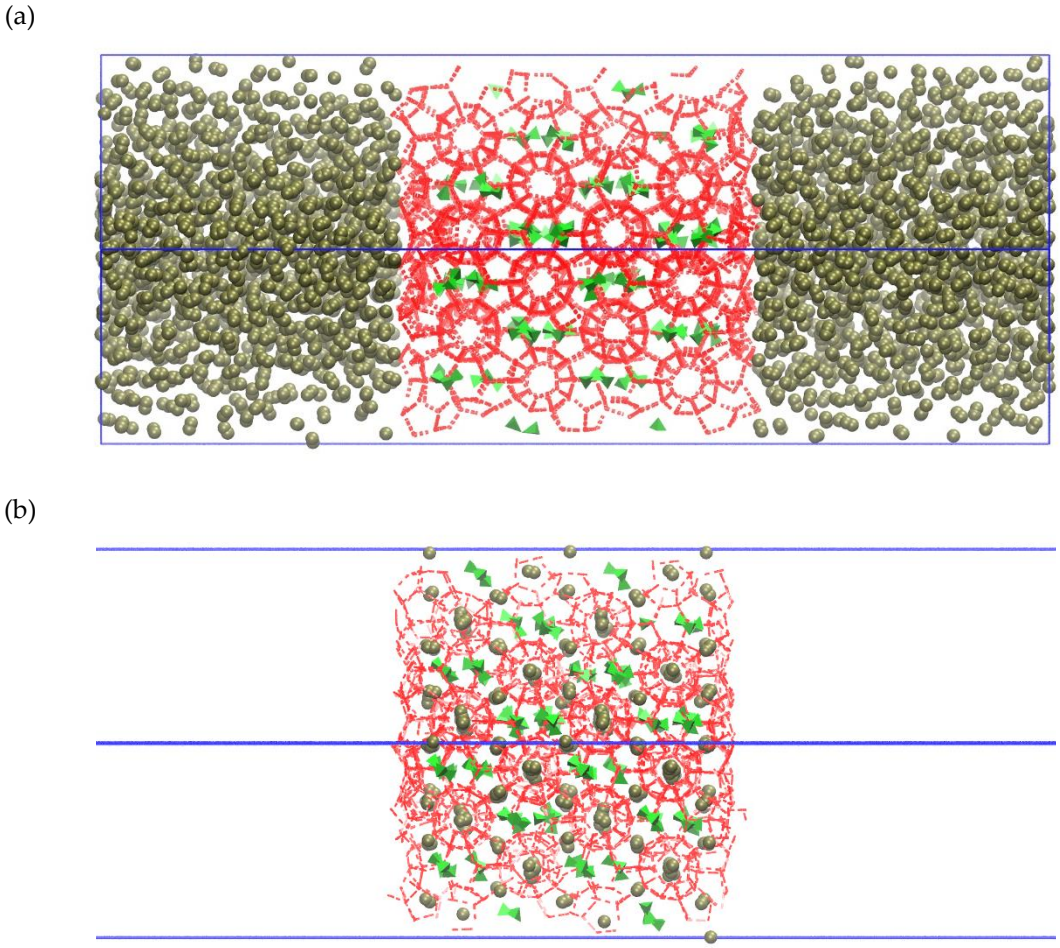

Figure 1. Illustration of two proposed models of propane/hydrogen hydrate uptake (**a**) and release (**b**) In this representation, each tri-group of light green octahedra denotes a propane molecule and olive-coloured spheres depict the hydrogen molecule position. Red dashed lines represent the hydrogen bond between water molecules.

Before starting the production NVT simulations, to let surrounding gas-phase hydrogen molecules fully cover the clathrate surfaces, an initial MD runs at 280 K for 200 ps, with applied position restraint on the water molecules of the hydrate. Subsequent NVT production simulations, at various temperatures (180–273 K) were performed over 500 ns for release and 2 µs for uptake study. Báez and Clancy The clathrate-liquid-ice recognition metrics were employed to distinguish geometrically between the encapsulated vs. free gas molecules [25]. The gas molecules with minimum 8 hydrate like water molecules categorized as encapsulated gas inside clathrate hydrate cage.

3. Experimental Methodology

The experimental apparatus for hydrate- formation included gas cylinders, a 316 stainless steel pressure vessel with approximately 340 cm^3, refrigerator to control the temperature of the vessel, tilting shaker to agitate the water inside the vessel and logging system to record the data during the formation time (Figure 2). Detailed information about the hydrate system is presented in our previous work [26]. Before each experiment, the vessel was sterilised using an ethanol solution (70 wt%). 10 cm^3 of deionised water was loaded into the vessel. The vessel closed, sealed and evacuated for 3 min to remove any residual air, and then pressurised to 4 bar using pure high purity propane gas. The cell was cooled down to 1.5 °C and kept at the desired temperature for 7 days to gauge the yield towards full

hydrate conversion. In the second step, 25 bar of hydrogen was loaded on the top of formed propane hydrate to study hydrogen uptake at (or very near) the desired temperature of 1.5 °C for 7 days.

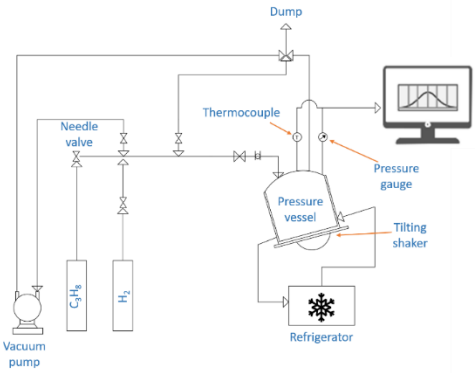

Figure 2. Schematic of the gas-hydrate rig. The four main sections are gas supplier, distribution terminal, reactor and refrigerator.

4. Results and Discussion

Form our previous study, the melting temperatures of T propane/hydrogen-clathrate surfaces were expected to be around 280 K [17]. The evolution in the number of hydrogen uptaken into/released from the propane hydrate was judged via the Báez–Clancy criteria, is specified in Figure 3 for both release and uptake at 180, 200, 220, 240, 260 and 273 K. Due to the observed slow kinetics of the uptake simulation, the simulation for hydrogen uptake extended up to 5 µs while for the case of release study a kind of plateau was observed after 500 ns. The rate constant of the gas uptake/release correlates directly with the simulation temperate as the thermal "driving forces" for gas diffusion.

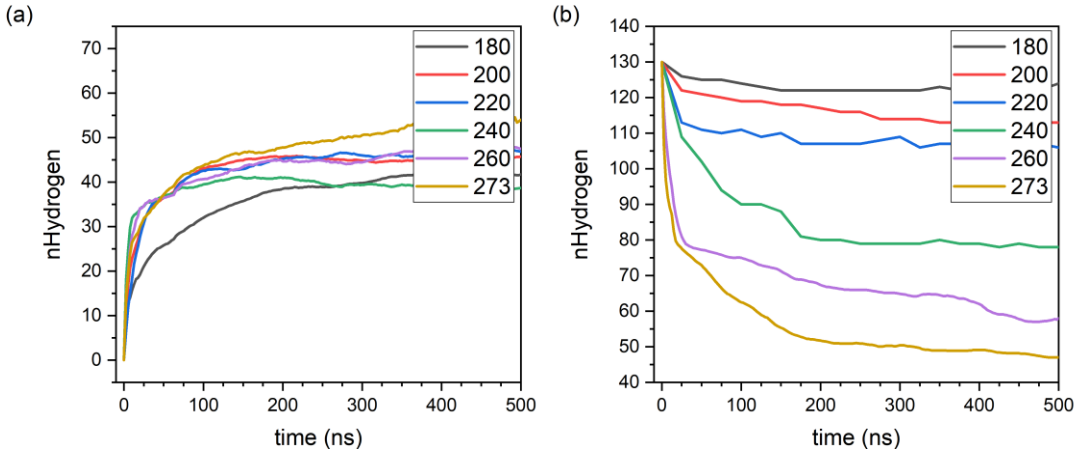

Figure 3. Hydrogen uptake (**a**) and release (**b**) in non-equilibrium simulations at various temperature.

The density map of molecules (water, propane and hydrogen) along the X-axis at different time stages can provide a better insight on the hydrate condition, the position of the propane molecules which can also be interpreted as the large-cage occupancy and the cage-filling pattern based on hydrogen diffusion in propane hydrate. Figure 4a illustrates the density map for hydrogen uptake in which hydrogen density in the range of 3.2 to 7.9 along X-axis at the starting time of the simulation (t = 0 ns) is zero while water distribution in this range is well distributed, due to the long-range order of clathrate hydrate. This order also can be observed in the case of propane molecules, those are located in large cages. During the simulation time, the water and propane distributions stay intact while the hydrogen penetrating the hydrate area and filling the first and second column of the small cages in hydrate structure. The existing plateau in Figure 3a after 250 ns for most of the

temperatures can also be noted in the similar density map of hydrogen at 250 and 500 ns. The main reason behind this similarity is attributable to the slow diffusion rate of the hydrogen molecules inside the hydrate structure. Internal hopping of hydrogen inside a hydrogen-hydrate lattice has been previously investigated by English and his colleagues [27,28], but in the case of propane/hydrogen hydrate, since all large cages are already occupied by propane molecules, the only available path for filling the whole hydrate is the small-to-small cage hopping which has to be done by pathing hydrogen molecule through a pentagonal ring.

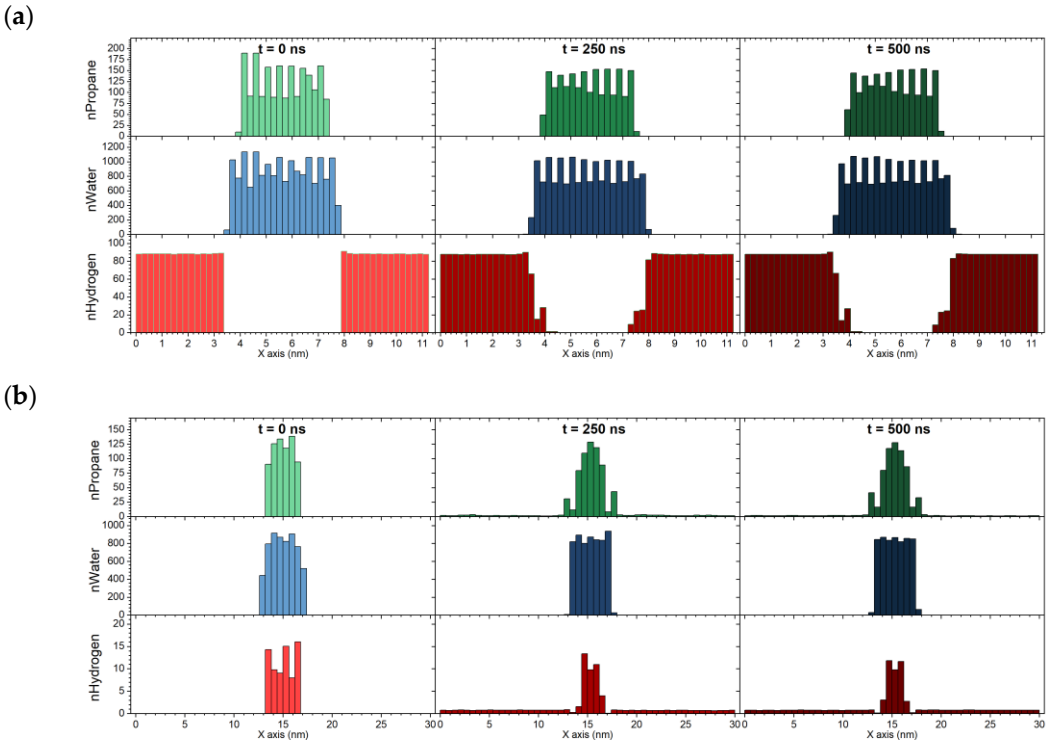

Figure 4. Density map of propane, water, and hydrogen molecules along the X-axis for uptake (**a**) and release (**b**).

The density map during hydrogen release simulation is illustrated in Figure 4b. Since for release study the hydrate is in contact with vacuum, some propane from the outer layer cages will be released into vacuum part. The presence of propane molecules can be seen in Figure 4b. A hydrogen molecule leaves its small cage, hops into another small cage in its neighbour and finds the way out from the hydrate lattice. The same limitation discussed on the difficulty of small-to-small hopping, the hydrogen exists in the centre of the hydrate lattice may never be able to leave the hydrate lattice.

To analyse the diffusion of the hydrogen molecules inside the hydrate structure, 300 sets of hydrogen molecules remaining in the hydrate structure over the whole sampling period (100 ns) were identified using Baez–Clancy method, and the MSD value of each set was calculated. The averaged MSD curve at each temperature for both uptake and release studies is illustrated in Figure 5 and the diffusion coefficient of each is listed in Table 1. It was found that the hydrogen molecules show a higher movement in the case of release studies in which the hydrate is in contact with a vacuum in compare with the uptake study where gas form hydrogen molecules are located on the top of the hydrate structure. This difference is caused following to the presence of some empty large cages due to the migration of propane molecules from the hydrate structure to the vacuum part. On the other hand, in uptake studies fully occupied large cages, all along the simulation time, limited movement of the infiltrated hydrogen molecules into hydrate structure resulted in a lower diffusion coefficient in this working condition. The activation energies of each diffusion scenario, in the presence and absence of

available large cages, release and uptake, are also calculated using the Arrhenius model based on the extracted diffusion coefficients at high temperatures (Table 1). Non-Arrhenius diffusion behaviour observed at lower temperatures can due to an enhanced local structural ordering [29]. In addition, at a lower temperature, the structure of the diffusion layer formed in a solid/gas interface also plays a significant role in the hydrogen uptake/release kinetics [30]. Further studies are required to explore the interfacial phenomena in gas hydrate systems.

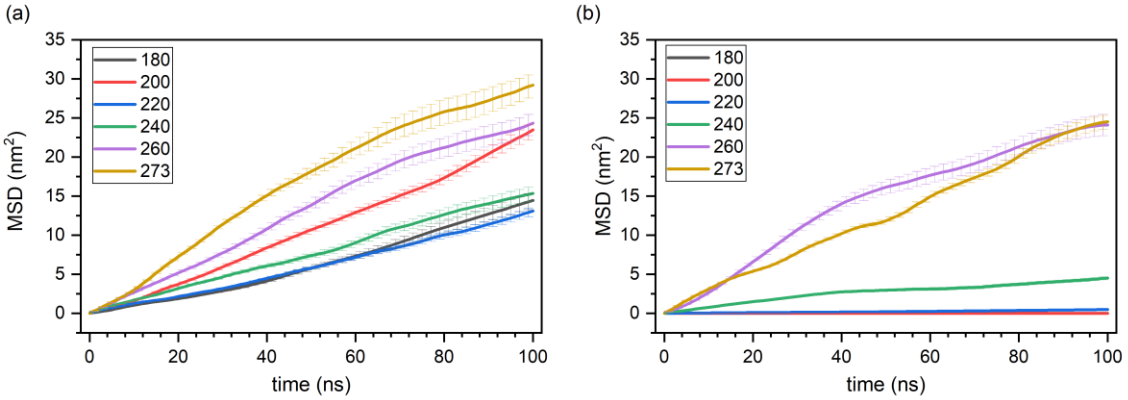

Figure 5. Mean-square displacement (MSD) curves of the hydrogen molecules in hydrate cages at various temperatures for both uptake (**a**) and release (**b**) simulation studies.

This result was confirmed in previous reports [28,31] showing the lower energy barrier for a small cage to a large cage diffusion in compare with the gas diffusion from a small cage to another small cage in a hydrate structure.

Table 1. The diffusion coefficient and the activation energy of the hydrogen molecules in hydrate cages at various temperatures for both uptake and release simulation studies.

Temp (K)	Diffusion Coefficient (10^{-5} cm^2/s)	
	Uptake	Release
180	0.0169	0.00002
200	0.0368	0.00003
220	0.0165	0.00066
240	0.0281	0.01226
260	0.0441	0.02897
273	0.0694	0.03813
Activation Energy (kJ/mol)	13.11 ± 1.11	44.80 ± 5.35

Hydrogen storage in clathrates was also studied experimentally in two steps. The first involved formation of pure hydrate, and second loading of pure hydrogen into the formed hydrate. There are two main categories in the design of the reactors used for hydrate formation, (I) water dispersion in which water dispersed in a cold high-pressure gas chamber [32–34] and (II) gas dispersion reactors where high-pressure gas introduces to a cold body of water. In this family gas/water mixture can be enhanced by bubbling [35–37] or different stirring techniques [38–40]. The designs with water dispersion found to be more suitable for hydrogen storage due to the formation of the small pieces of hydrates which will provide sufficient free surfaces for hydrogen uptake or release. Many designs are dispersing gas in a large volume of water, which is useful for many other applications such as water treatment or dewatering. The formation of a big slab of hydrate will make it unsuitable for hydrogen storage application. An extra step of hydrate crashing is being used for gas adsorption/desorption application.

Figure 6a presents the reactor used to hydrate formation in this study. This reactor works based on gas dispersion mechanism for hydrate formation which means the gas will be purged into already

loaded water at low temperature and after a while, the hydrate will nucleate and start growing on the wall and bottom of the reactor and at the end of the formation reaction, a solid, dense and large part of the hydrate will form (Figure 6b,c). The number of adsorbed propane molecules during the first step (hydrate formation) was calculated based on the pressure drop and compressibility factor of propane molecule at the temperature and pressure hydrate formation condition (Figure 6d,e). Since 10 mL of water was loaded into the reactor the expected adsorbed propane molecule after the full formation of type-II hydrate will be equal to 0.032 mol. This means although no water in liquid form remained in the reactor, only 73% of expected gas was adsorbed during hydrate formation. This difference can be explained by two main reasons: (1) a small minority of formed large cages stayed un-occupied and (2) some possible water in liquid form is stocked in between two formed hydrate chunks. On the other hand, the ratio between the amounts of adsorbed hydrogen over adsorbed propane is around 2.42, as compared to an expected value 2 based on type II hydrate (assuming one H_2 molecule per small cage). This higher adsorption of the hydrogen is in agreement with the first assumption mentioned above regarding formation of propane hydrate with a small minority of empty large cages. This means that a part of the adsorbed hydrogen fills, in part, the available large cages, e.g., with double occupation a likelihood at present pressures in the general range of 20–30 bar.

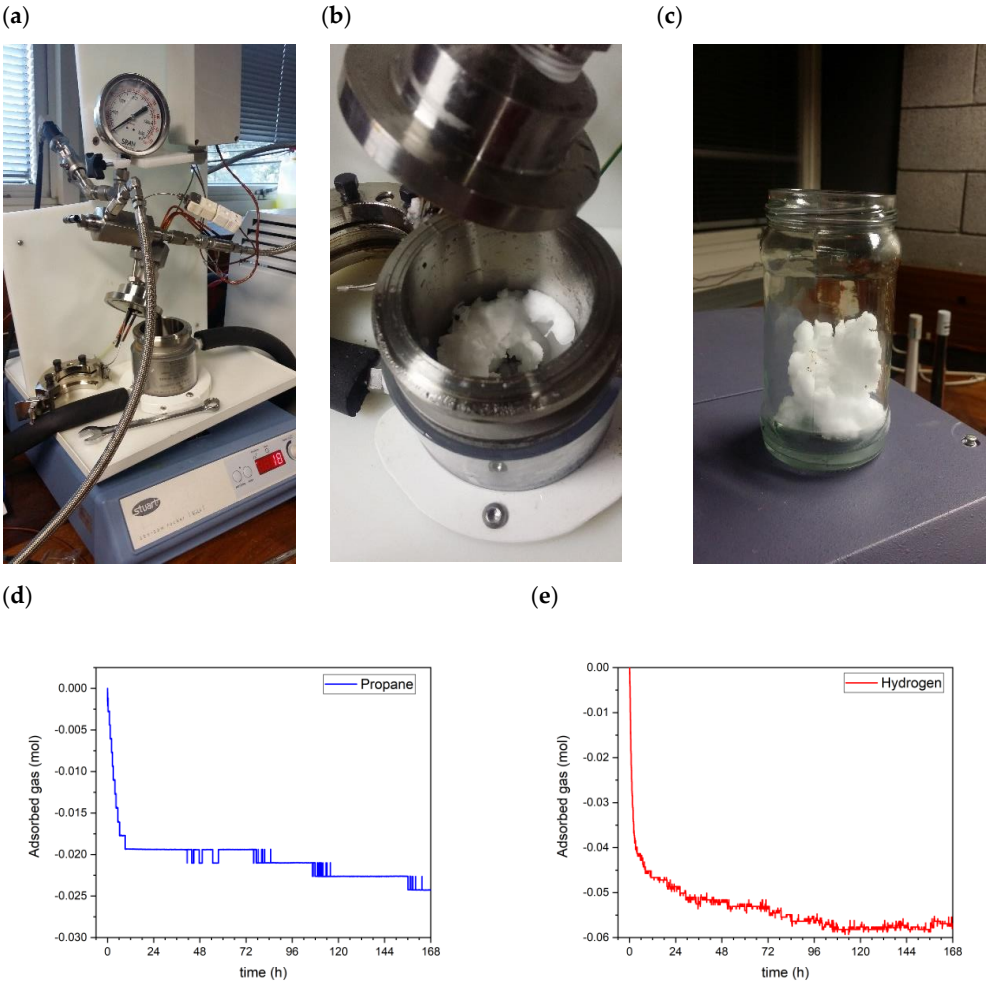

Figure 6. (**a**) High-pressure apparatus used for hydrogen growth and hydrogen storage study, (**b**,**c**) the formed hydrate immediate after pressure release and opening the reactor, (**d**) Number of propane moles adsorbed during the formation of the hydrate in the first 7 days under 4 bar pressure of propane, (**e**) Number of hydrogen moles adsorbed during the storage step in the second 7 days under 25 bar pressure of hydrogen at 1.5 °C.

On the other hand, the maximum hydrogen storage capacity of a fully occupied type II gas hydrate, 8 propane and 16 hydrogen molecules in a unit cell with 136 water molecules will be 1.13 wt%. This value can increase in the case of partial occupancy of propane in the large cages (Table 2). Based on the number of adsorbed hydrogen and propane molecules in the hydrate formed using 10 mL of water, the overall hydrogen stored in the formed propane hydrate is about 1.04 wt%. This observation also supports the second assumption regarding the existence of liquid-form water trapped on the surface of between formed hydrate chunks. It is worth mentioning that the higher observed value vis-a-vis the previously reported values of hydrogen storage in C_3H_8+H_2 hydrate, 0.33% at 270 K [41], and 0.04% at 263 K [42] is due to lower selected working temperature. According to our MD results, the diffusion coefficient at 273 K (0.0694×10^{-5} cm^2/s) is approximately 1.5 times larger than that of 260 K (0.0441×10^{-5} cm^2/s), suggesting a strong dependence of the uptake rate on temperature.

Table 2. Estimated-hydrogen storage capacity with respect to the large-cage occupancy.

Large Cages Occupancy (%)	Water Molecules	Propane Molecules	Hydrogen Molecules	Storage Capacity (wt%)
100	1360	80	160	1.13%
95	1360	76	172	1.22%
90	1360	72	184	1.31%
85	1360	68	196	1.41%
80	1360	64	208	1.50%
75	1360	60	220	1.60%
70	1360	56	232	1.69%

5. Conclusions

In this study, propane/hydrogen mixed hydrate (sII structure) was chosen as a suitable hydrate for hydrogen storage with ideal 1.13 wt% storage capacity. Required non-equilibrium MD simulations were conducted to analyse hydrogen release and uptake from/into propane planar clathrate surfaces at 180–273 K. The observed surface fully treated hydrate models from a simulation study, in addition to, the visual inspection of formed hydrate beside lower hydrogen storage capacity for the formed hydrate (1.04 wt%) in experiments, proved the requirement of forming hydrates with the maximum surface to volume ratio to be able to maximise the storage capacity as well as the gas uptake kinetics. As a result, we advocate the use of liquid-dispersion reactors, featuring a water-injection system into a cold gas chamber at high pressure, as opposed to the use of gas-dispersion (fixed-bed) reactors.

In future work, detailed (and possibly time-dependent) measurement and characterisation grain size of hydrate would be useful, in terms of estimating growth rates of the C_3H_8+H_2 hydrate more accurately. These results could be compared with results obtained from molecular dynamics.

Author Contributions: M.R.G., S.T. and N.J.E. conceived the study conceptually. M.R.G. did the experimental and simulations. S.T. and N.J.E. contributed importantly with an interpretation of results. All authors have read and agreed to the published version of the manuscript.

Funding: This research was funded by Irish Research Council (GOIPD/2016/365) and Science Foundation Ireland 15/ERC-I3142.

Acknowledgments: M.R.G. and N.J.E. thank the Irish Research Council and Science Foundation Ireland for their funding.

Conflicts of Interest: The authors declare no conflict of interest.

References

1. Makogon, I.F. *Hydrates of Hydrocarbons*; Pennwell Books: Tulsa, OK, USA, 1997; ISBN 0878147187.
2. Veluswamy, H.P.; Kumar, R.; Linga, P. Hydrogen storage in clathrate hydrates: Current state of the art and future directions. *Appl. Energy* **2014**, *122*, 112–132. [CrossRef]

3. Mao, W.L.; Mao, H.-K. Hydrogen storage in molecular compounds. *Proc. Natl. Acad. Sci. USA* **2004**, *101*, 708–710. [CrossRef] [PubMed]
4. Sandford, S.; Allamandola, L.; Geballe, T.; Mao, H.-K.; Hemley, R.J.; Hu, J.; Shu, J.; Hemley, R.J.; Somayazulu, M.; Zhao, Y. Spectroscopic detection of molecular hydrogen frozen in interstellar ices. *Science* **1993**, *262*, 400–402. [CrossRef] [PubMed]
5. Di Profio, P.; Arca, S.; Rossi, F.; Filipponi, M. Comparison of hydrogen hydrates with existing hydrogen storage technologies: Energetic and economic evaluations. *Int. J. Hydrogen Energy* **2009**, *34*, 9173–9180. [CrossRef]
6. Shibata, T.; Yamachi, H.; Ohmura, R.; Mori, Y.H. Engineering investigation of hydrogen storage in the form of a clathrate hydrate: Conceptual designs of underground hydrate-storage silos. *Int. J. Hydrogen Energy* **2012**, *37*, 7612–7623. [CrossRef]
7. Nakayama, T.; Tomura, S.; Ozaki, M.; Ohmura, R.; Mori, Y.H. Engineering Investigation of Hydrogen Storage in the Form of Clathrate Hydrates: Conceptual Design of Hydrate Production Plants. *Energy Fuels* **2010**, *24*, 2576–2588. [CrossRef]
8. Florusse, L.J.; Peters, C.J.; Schoonman, J.; Hester, K.C.; Koh, C.A.; Dec, S.F.; Marsh, K.N.; Sloan, E.D. Stable low-pressure hydrogen clusters stored in a binary clathrate hydrate. *Science* **2004**, *306*, 469–471. [CrossRef]
9. Lee, H.; Lee, J.; Kim, D.Y.; Park, J.; Seo, Y.-T.; Zeng, H.; Moudrakovski, I.L.; Ratcliffe, C.I.; Ripmeester, J.A. Tuning clathrate hydrates for hydrogen storage. *Nature* **2005**, *434*, 743–746. [CrossRef]
10. Mao, W.L.; Mao, H.; Goncharov, A.F.; Struzhkin, V.V.; Guo, Q.; Hu, J.; Shu, J.; Hemley, R.J.; Somayazulu, M.; Zhao, Y. Hydrogen Clusters in Clathrate Hydrate. *Science* **2002**, *297*, 2247–2249. [CrossRef]
11. Hasegawa, T.; Brumby, P.E.; Yasuoka, K.; Sum, A.K. Mechanism for H 2 diffusion in sII hydrates by molecular dynamics simulations. *J. Chem. Phys.* **2020**, *153*, 054706. [CrossRef]
12. Skiba, S.S.; Larionov, E.G.; Manakov, A.Y.; Kolesov, B.A.; Ancharov, A.I.; Aladko, E.Y. Double clathrate hydrate of propane and hydrogen. *J. Incl. Phenom. Macrocycl. Chem.* **2009**, *63*, 383–386. [CrossRef]
13. English, N.J.; MacElroy, J.M.D. Perspectives on molecular simulation of clathrate hydrates: Progress, prospects and challenges. *Chem. Eng. Sci.* **2015**, *121*, 133–156. [CrossRef]
14. Huang, Y.; Zhu, C.; Wang, L.; Cao, X.; Su, Y.; Jiang, X.; Meng, S.; Zhao, J.; Zeng, X.C. A new phase diagram of water under negative pressure: The rise of the lowest-density clathrate s-III. *Sci. Adv.* **2016**, *2*, e1501010. [CrossRef] [PubMed]
15. Ghaani, M.R.; English, N.J. Molecular-dynamics study of propane-hydrate dissociation: Fluctuation-dissipation and non-equilibrium analysis. *J. Chem. Phys.* **2018**, *148*, 114504. [CrossRef]
16. Ghaani, M.R.; English, N.J. Molecular Dynamics Study of Propane Hydrate Dissociation: Nonequilibrium Analysis in Externally Applied Electric Fields. *J. Phys. Chem. C* **2018**, *122*, 7504–7515. [CrossRef]
17. Ghaani, M.R.; English, N.J. Hydrogen-/propane-hydrate decomposition: Thermodynamic and kinetic analysis. *Mol. Phys.* **2019**, 1–9. [CrossRef]
18. Wang, J.; Wolf, R.M.; Caldwell, J.W.; Kollman, P.A.; Case, D.A. Development and testing of a general amber force field. *J. Comput. Chem.* **2004**, *25*, 1157–1174. [CrossRef]
19. Cornell, W.D.; Cieplak, P.; Bayly, C.I.; Kollman, P.A. Application of RESP charges to calculate conformational energies, hydrogen bond energies, and free energies of solvation. *J. Am. Chem. Soc.* **1993**, *115*, 9620–9631. [CrossRef]
20. Alavi, S.; Ripmeester, J.A.; Klug, D.D. Molecular-dynamics study of structure II hydrogen clathrates. *J. Chem. Phys.* **2005**, *123*, 024507. [CrossRef]
21. Essmann, U.; Perera, L.; Berkowitz, M.L.; Darden, T.; Lee, H.; Pedersen, L.G. A smooth particle mesh Ewald method. *J. Chem. Phys.* **1995**, *103*, 8577–8593. [CrossRef]
22. Allen, M.P.; Tildesley, D.J. *Computer Simulation of Liquids*; Oxford University Press: Oxford, UK, 2017; ISBN 0192524704.
23. Udachin, K.A.; Lu, H.; Enright, G.D.; Ratcliffe, C.I.; Ripmeester, J.A.; Chapman, N.R.; Riedel, M.; Spence, G. Single crystals of naturally occurring gas hydrates: The structures of methane and mixed hydrocarbon hydrates. *Angew. Chem. Int. Ed.* **2007**, *46*, 8220–8222. [CrossRef] [PubMed]
24. Rahman, A.; Stillinger, F.H. Proton Distribution in Ice and the Kirkwood Correlation Factor. *J. Chem. Phys.* **1972**, *57*, 4009–4017. [CrossRef]
25. Bernal, J.D.; Fowler, R.H. A Theory of Water and Ionic Solution, with Particular Reference to Hydrogen and Hydroxyl Ions. *J. Chem. Phys.* **1933**, *1*, 515–548. [CrossRef]

26. Ghaani, M.R.; English, N.J.; Allen, C.C.R. Magnetic-Field Manipulation of Naturally Occurring Microbial Chiral Peptides to Regulate Gas-Hydrate Formation. *J. Phys. Chem. Lett.* **2020**, 9079–9085. [CrossRef] [PubMed]
27. Burnham, C.J.; English, N.J. Free-Energy Calculations of the Intercage Hopping Barriers of Hydrogen Molecules in Clathrate Hydrates. *J. Phys. Chem. C* **2016**, *120*, 16561–16567. [CrossRef]
28. Burnham, C.J.; Futera, Z.; English, N.J. Quantum and classical inter-cage hopping of hydrogen molecules in clathrate hydrate: Temperature and cage-occupation effects. *Phys. Chem. Chem. Phys.* **2017**, *19*, 717–728. [CrossRef] [PubMed]
29. Wang, T.; Zhang, F.; Yang, L.; Fang, X.W.; Zhou, S.H.; Kramer, M.J.; Wang, C.Z.; Ho, K.M.; Napolitano, R.E. A computational study of diffusion in a glass-forming metallic liquid. *Sci. Rep.* **2015**, *5*, 10956. [CrossRef]
30. Aman, Z.M.; Koh, C.A. Interfacial phenomena in gas hydrate systems. *Chem. Soc. Rev.* **2016**, *45*, 1678–1690. [CrossRef]
31. Cao, H.; English, N.J.; MacElroy, J.M.D. Diffusive hydrogen inter-cage migration in hydrogen and hydrogen-tetrahydrofuran clathrate hydrates. *J. Chem. Phys.* **2013**, *138*, 094507. [CrossRef]
32. Ohmura, R.; Kashiwazaki, S.; Shiota, S.; Tsuji, H.; Mori, Y.H. Structure-I and Structure-H Hydrate Formation Using Water Spraying. *Energy Fuels* **2002**, *16*, 1141–1147. [CrossRef]
33. Tsuji, H.; Ohmura, R.; Mori, Y.H. Forming Structure-H Hydrates Using Water Spraying in Methane Gas: Effects of Chemical Species of Large-Molecule Guest Substances. *Energy Fuels* **2004**, *18*, 418–424. [CrossRef]
34. Li, G.; Liu, D.; Xie, Y.; Xiao, Y. Study on Effect Factors for CO 2 Hydrate Rapid Formation in a Water-Spraying Apparatus. *Energy Fuels* **2010**, *24*, 4590–4597. [CrossRef]
35. Takahashi, M.; Kawamura, T.; Yamamoto, Y.; Ohnari, H.; Himuro, S.; Shakutsui, H. Effect of Shrinking Microbubble on Gas Hydrate Formation. *J. Phys. Chem. B* **2003**, *107*, 2171–2173. [CrossRef]
36. Havelka, P.; Linek, V.; Sinkule, J.; Zahradník, J.; Fialova, M. Effect of the ejector configuration on the gas suction rate and gas hold-up in ejector loop reactors. *Chem. Eng. Sci.* **1997**, *52*, 1701–1713. [CrossRef]
37. Xin, Y.; Zhang, J.; He, Y.; Wang, C. Modelling and experimental study of hydrate formation kinetics of natural gas-water-surfactant system in a multi-tube bubble column reactor. *Can. J. Chem. Eng.* **2019**, *97*, 2765–2776. [CrossRef]
38. Hould, N.; Elanany, M.S.; Aleisa, R.M.; Al-Majnouni, K.A.; Al-Malki, A.; Abba, I. Evaluating polymeric inhibitors of ethane clathrate hydrates. *J. Nat. Gas Sci. Eng.* **2015**, *24*, 543–549. [CrossRef]
39. Vysniauskas, A.; Bishnoi, P.R. A kinetic study of methane hydrate formation. *Chem. Eng. Sci.* **1983**, *38*, 1061–1072. [CrossRef]
40. Tang, L.-G.; Li, X.-S.; Feng, Z.-P.; Lin, Y.-L.; Fan, S.-S. Natural Gas Hydrate Formation in an Ejector Loop Reactor: Preliminary Study. *Ind. Eng. Chem. Res.* **2006**, *45*, 7934–7940. [CrossRef]
41. Park, J.; Lee, H. Spectroscopic evidences of the double hydrogen hydrates stabilized with ethane and propane. *Korean J. Chem. Eng.* **2007**, *24*, 624–627. [CrossRef]
42. Abbondondola, J.A.; Fleischer, E.B.; Janda, K.C. Comparative study of hydrogen, argon, and xenon uptake into a propane hydrate. *AIChE J.* **2010**, *56*, 2734–2741. [CrossRef]